BUTTERWORTH HEINEMANN

NDT&E International, Vol. 28, No. 2, pp. 73–82, 1995

0963-8695(94)00005-0
0963-8695/95 $10.00 + 0.00

Characterization of texture and residual stress in a section of 610 mm pipeline steel

L. Clapham*, T. W. Krause*, H. Olsen*, B. Ma*, D. L. Atherton*, P. Clark† and T. M. Holden‡

*Applied Magnetics Group, Department of Physics, Queen's University, Kingston, Ontario, K7L 3N6, Canada
†Materials and Metallurgical Engineering Department, Queen's University, Kingston, Ontario, K7L 3N6, Canada
‡AECL Research, Chalk River, Ontario, K0J 1J0, Canada

Received 3 February 1994; revised 2 November 1994

Gas pipelines are inspected for defects such as corrosion. The most commonly used nondestructive inspection tool uses the magnetic flux leakage (MFL) technique. The MFL signals depend on the magnetic behaviour of the pipe, which is sensitive to its microstructure and crystallographic texture as well as both residual and applied stresses. Here a section of commercial X70 pipeline is characterized using microstructural examination, X-ray diffraction (to determine crystallographic texture) and neutron diffraction (for residual stress measurement). The results correlate well with the manufacturing steps used for this type of pipe. Magnetic characterization is also performed using magnetic Barkhausen noise measurements, which reflect the magnetic anisotropy in the pipe and thus the MFL signal. These results do not correlate simply with crystallographic texture and residual strain results, but this is not unexpected given the complex nature of the material and its stress state.

Keywords: pipeline steel, microstructure, residual stress

Modern gas transmission pipelines are essentially pressure vessels, operating at up to 70% of their yield strength. As they age in service they may develop defects associated with general or localized corrosion and environmentally induced cracking. Safety, environmental and economic considerations dictate that these defects be located and removed or repaired before failure occurs. The most commonly used methods of nondestructive pipeline inspection are based on the magnetic flux leakage (MFL) technique[1,2]. This involves magnetizing the pipe wall to a near-saturation flux density, and then detecting the leakage flux near the pipe wall using Hall probes or induction coils. Irregularities in the pipe wall create anomalies in this leakage flux signal, allowing defects to be located. More recently, emphasis in pipeline inspection has shifted from simply locating defects to the accurate determination of their severity, the aim being to estimate wall thickness losses to within 10%[3,4]. This capability allows maximum allowable operating pressure calculations to be made directly, based on the MFL result.

The magnetic behaviour and hence the MFL signals obtained when inspecting an in-service steel pipe is influenced strongly by the magnetic texture of the pipe and its stress state. Both of these factors depend in turn on the processing and stress histories. Magnetic texture is influenced by the magnetic anisotropy in the pipe, which depends on the magnetocrystalline anisotropy and on the angular distribution of the easy magnetization axes of individual steel grains. In an unstressed steel grain this easy axis lies along the $\langle 100 \rangle$ crystal direction[5], and thus the crystallographic texture plays a significant role. The application of stress may alter this magnetic texture, since under tension magnetostrictive effects will tend to realign domain vectors with those $\langle 100 \rangle$ directions most closely parallel to the stress axis[5].

The stress state of the pipe is important not only because of its influence on magnetic parameters and MFL signals[6,7], but also because exceeding the stress limit can have serious consequences. Residual stresses may make a significant contribution to the total stress in a pressurized pipeline, since the combination of residual and applied stress may locally exceed the ultimate tensile stress. This is of particular concern in those regions where defects act as stress raisers.

In the present study the residual stress, crystallographic and magnetic texture were examined in a 610 mm (24″) diameter pipeline section. Neutron diffraction allowed small-scale strain measurements to be made through the thickness of the pipe wall; in addition a residual stress map was determined for a surface region near an artificially produced 'defect'. X-ray diffraction was used to establish the crystallographic texture in the pipe. Finally, magnetic Barkhausen noise (MBN) measurements were carried out to examine the influence of crystallographic texture and residual stress on the magnetic response of the material. A brief description of the MBN technique is provided in the experimental section.

Experimental

Pipeline sample

The sample used in this study was a 102 mm (4″) wide semicircular hoop section cut from a 610 mm (24″) diameter X70 steel pipe of 9 mm thickness with a yield strength 600 MPa. The cut was made through the weld region on one side, the other cut being 180° from the weld. The steel composition is given in Table 1. A corrosion pit-type defect was simulated by drilling a 13 mm diameter blind hole (50% penetration) in the outside pipe wall, at a position halfway between the two cut ends (this defect was of interest for a concurrent study of applied stress[8]). The region surrounding this defect was that selected for the residual stress map.

The amount of spring back on cutting the circular pipe section was noted as 6.7 mm. The semicircular pipe section had a smaller diameter than the original pipe diameter and, therefore, the spring back was associated with the relaxation of a compressive hoop stress present on the outside of the original full section. Extrapolation from applied stress measurements[8] determined that the outside surface of the pipe was originally under a compressive hoop stress of 30 MPa. Samples for metallographic examination were taken from one end of the semicircular pipe section. Cross-sectional samples parallel to the pipe axis (*ie* the original plate rolling direction) were prepared using standard grinding and polishing techniques, and were etched using a 2% Nital solution.

Table 1. Composition (in wt%) of X70 pipeline steel used in this study

C	Mn	P	S	Si	V	Ti	Nb
0.12	1.46	0.02	0.003	0.22	0.060	0.020	0.040

Residual stress measurement

A general description of the use of neutron diffraction for residual stress measurement can be found elsewhere[9,10]. In the pipeline sample, residual stresses were calculated from residual strain measurements made in the hoop, radial (*ie* through-thickness) and axial (*ie* pipe axis) directions. These residual strain measurements were made using the neutron diffraction facilities at the NRU reactor located in the AECL laboratory in Chalk River, Canada. The L3 triple axis crystal spectrometer was used, employing the (115) planes of a Ge monochromator to provide a neutron beam of $\lambda = 1.465$ Å. The diffraction volume was defined by 1.5 mm horizontal and vertical slits, resulting in a gauge volume of $\sim 3.4\ \text{mm}^3$. Strain was measured using the Fe (112) reflection.

The angular position (2θ) of the diffracted peak was determined by fitting a Gaussian profile to the data. θ was then used to determine the value of d, the lattice parameter, using Bragg's law:

$$\lambda = 2d_{112} \sin \theta_{112}$$

In order to obtain the strain from a measured d value, an 'unstrained' reference spacing was obtained by averaging the d_{112} spacings of a small (10 mm × 5 mm × 5 mm) piece of the pipe in the three directions (hoop, radial and axial). This reference spacing was found to be 1.1705 Å. The residual strain (ε) was then calculated from:

$$\varepsilon = \frac{d - d_{\text{ref}}}{d_{\text{ref}}}$$

The residual strains in the hoop (H), axial (A) and radial (R) directions were then used to calculate residual stress using:

$$\sigma_i = \frac{E}{(1+\nu)}\left[\varepsilon_i + \frac{\nu}{(1-2\nu)}(\varepsilon_A + \varepsilon_H + \varepsilon_R)\right]$$

The diffraction elastic constants E (Young's modulus) and ν (Poisson's ratio) were 225 and 0.276, respectively. These values were calculated according to the method of Kroner[11,12] from the single crystal constraints for iron[13]. The Kroner model allows for continuity in stress and strain at the boundaries of spherical grains, and is more appropriate for lattice strains measured using neutron diffraction.

Texture measurements

Sample texture was determined using X-ray diffraction pole figures. Four surfaces (all parallel to the pipe surface) were prepared for this purpose: the outside surface, the inside surface and surfaces at depths of 3.5 and 6 mm below the outside. (110), (200) and (112) pole figures were obtained in each case.

Magnetic Barkhausen noise measurements

The application of a varying magnetic field induces small discontinuous magnetization changes in a ferromagnetic material, due to domain walls moving abruptly from one pinning site to another and abrupt rotation of the domain magnetization vector. The associated voltages induced in a pickup coil on the sample are referred to as magnetic Barkhausen noise (MBN). MBN has been related to a number of metallurgical parameters such as grain size and carbon content[14,15]. Both elastic and plastic deformation may also influence MBN[16,17]. Elastic deformation, as mentioned earlier, modifies the energetically favourable domain configuration, whereas plastic deformation produces regions of high dislocation density which may act as domain wall pinning sites. In pipeline steels the processing steps usually result in a rather complex and ill-defined crystallographic texture and stress state. The magnetic anisotropy (*eg* the magnetic easy axis), which is dependent both on stress and crystallographic influences, can be investigated by evaluating the MBN as a function of sweep field orientation (with respect to the pipe axis)[18].

MBN measurements were performed using the experimental apparatus shown in Figure 1, which illustrates the ferrite-core sweep field magnet and pickup coil location. The signal to the sweep field coil was produced by a waveform generator and amplified with a bipolar power supply (sweep field frequency 12 Hz, amplitude ± 1.0 T). The MBN signal detected by the pickup coil was passed through a preamplifier (gain 5000) and a band-pass filter (3–200 kHz) before being displayed on a personal computer with a resident digital oscilloscope board (Computerscope). Skin depth calculations indicated that the samples were fully magnetized (skin depth, 3 mm); however, an analysis of the frequency spectrum of the MBN signal indicated that the majority of the MBN signal came from a depth of 0.025 mm to 0.7 mm.

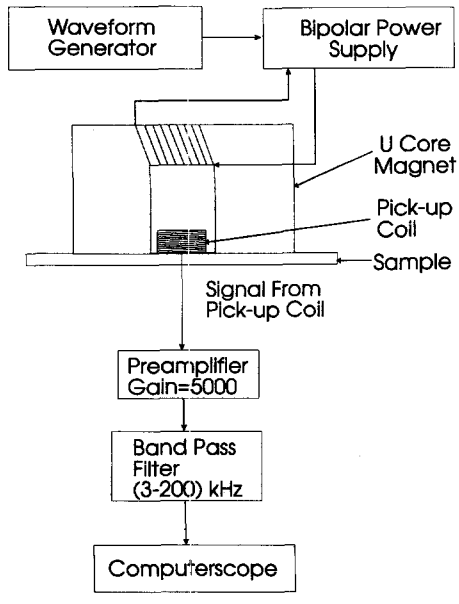

Figure 1 Schematic illustration of MBN measurement apparatus

MBN was sampled every 3 μs with a buffer size of 8 K. The sampling time of a single trace was 20 ms, with eight traces taken at each point. Analysis of the data involved deriving a V_{rms} for the (average) signal envelope, and a MBN energy signal which was interpreted as the area below the voltage^2 *vs* time spectrum.

MBN measurements of magnetic anisotropy were performed on the same surfaces for which X-ray pole figures had been obtained. For each sample, the sweep field magnet and pickup coil were rotated through 360° at 15° intervals. These MBN *vs* orientation results were then reduced to a 0°–180° range by averaging equivalent angles of the sweep field. The magnetic texture of each sample was characterized by a dimensionless parameter κ[18], where:

$$\kappa = \frac{V_{rms}(\max) - V_{rms}(\min)}{V_{rms}(\max) + V_{rms}(\min)}$$

$V_{rms}(\max)$ and $V_{rms}(\min)$ are the maximum and minimum rms voltages, respectively, measured over 180°.

Results and discussion

Optical microscopy

Optical examination of the microstructure revealed a uniformly fine grained material containing pearlite banding typical of a commercial controlled-rolled steel, Figure 2(a). The steel was relatively 'clean', with a low inclusion count. Of particular interest was the micro-

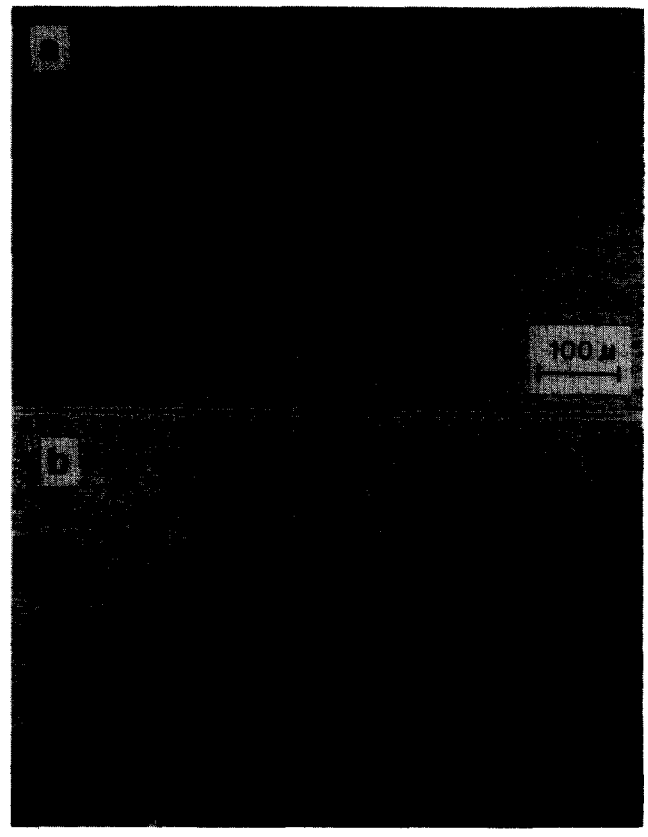

Figure 2 Longitudinal sections illustrating pipe wall microstructure: (a) from wall centre; (b) from near the pipe outer wall

structure at the outside surface of the pipe. Figure 2(b) shows the pearlite bands in some regions near the surface to be bent into a semicircular shape, indicative of compression-type plastic deformation at localized points on the surface. These regions were periodic (with a periodicity of ~1 mm) and were not associated with any obvious surface macroindentation. No such regions were observed on the inside surface of the pipe.

Texture measurements

The (110) X-ray pole figures obtained from the four sections through the pipe wall are shown in Figures 3(a)–(d) (note: for brevity only the (110) pole figure is shown). The two sections prepared from the middle of the pipe wall both display a strong texture characteristic of rolling with subsequent recrystallization, Figures 3(b) and (c)[19]. Neither the outside (Figure 3(a)) nor inside (Figure 3(d)) surfaces exhibit this recrystallized texture; rather, these pole figures suggest a weaker, unrecrystallized shear-type texture associated with the rolling process. The difference in texture between the centre and surfaces of the pipe wall implies that during the final rolling passes the plate temperature was too low to enable recrystallization at the two external surfaces (this is a situation which is generally considered to be undesirable).

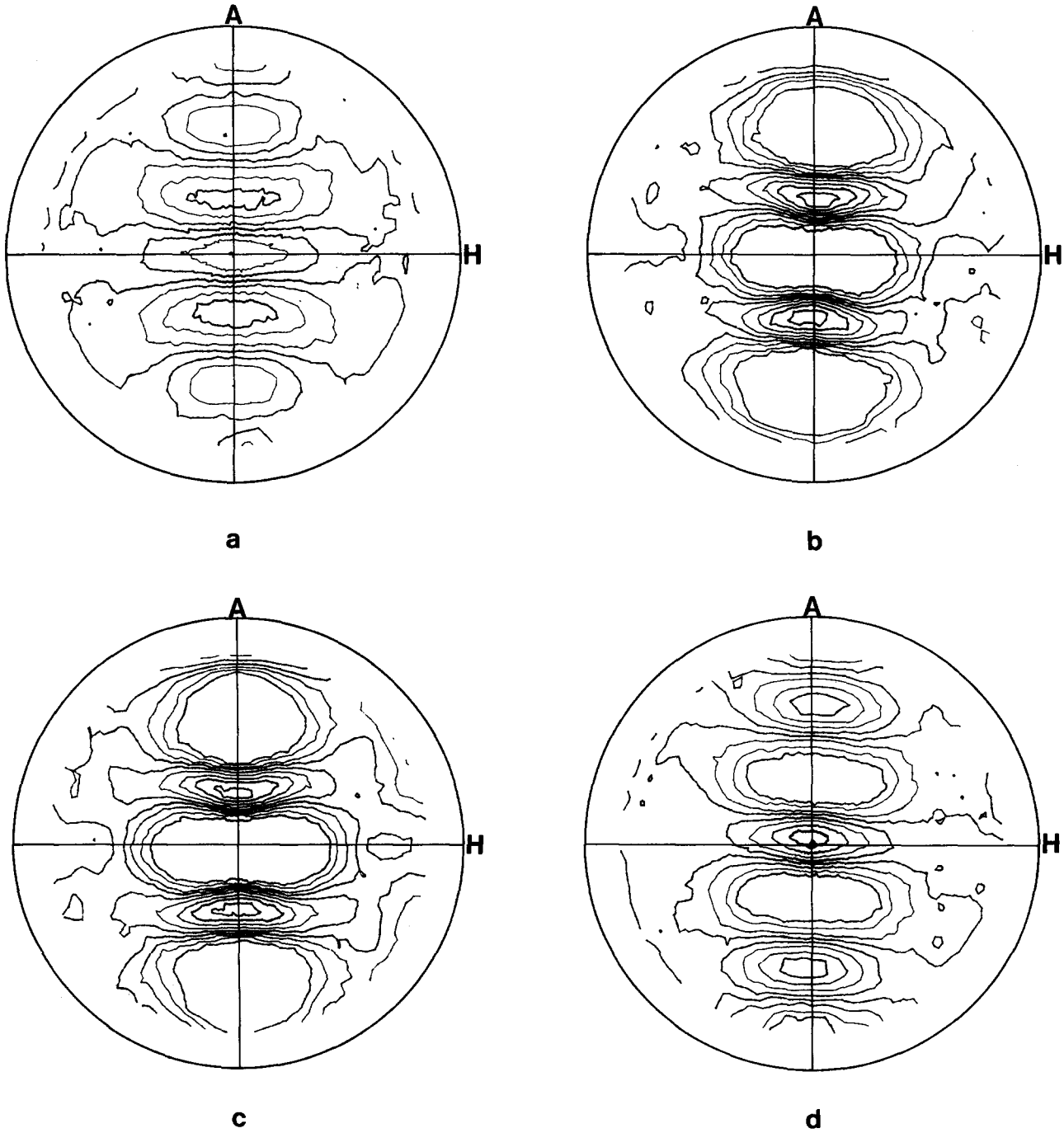

Figure 3 X-ray pole figures for the four surfaces through the pipe wall: (a) outside wall surface, (b) 3.5 mm below outside surface, (c) 6 mm below outside surface, (d) inside wall surface. *A* = axial direction, *H* = hoop direction, centre is the radial direction

Residual stress measurements

Residual strain measurements were made at 1–2 mm step intervals through the thickness of the pipe wall, both directly underneath the defect and also in a region remote from the defect (at least 40 mm away). Figure 4 summarizes the resulting through-thickness residual stresses in the hoop, axial and radial directions respectively in a region remote from the defect (similar results were found beneath the defect, and therefore they are not included as a separate graph). Of the three directions, the most significant residual stress gradient occurs for the axial direction, with a strongly compressive stress of ~100 MPa at the outside, rising to slightly tensile and finally zero stress close to the inside surface of the pipe wall.

To examine local variations in residual stress on the outside surface of the pipe, a 2D map of residual stress was made in the vicinity of the defect. Figure 5 indicates the loci of measurement positions surrounding the defect. All of these measurements were obtained from the region just below the outer pipe surface (from the outside wall to a depth of ~2 mm). Results for the hoop, axial and radial residual stresses are presented in the form of axial (y) scans at fixed hoop (x) positions in Figures 6(a), (b) and (c), respectively. These figures indicate that the axial stress is consistently compressive over the mapped region, with tensile stress in the hoop and radial directions. While the radial residual stress exhibits very little variation with position, both the hoop and axial residual stresses vary by up to 50 MPa. This variation is significant, particularly given the small size of the mapping zone (~15 × 20 mm). Furthermore, a comparison of Figure 6

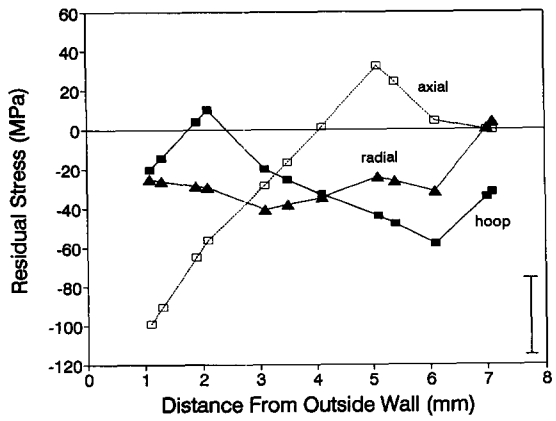

Figure 4 Experimentally determined through-thickness variation of residual hoop (-■-), axial (-□-) and radial (-▲-) stress. Uncertainty ~ ±20 MPa, shown as a single error bar on graph

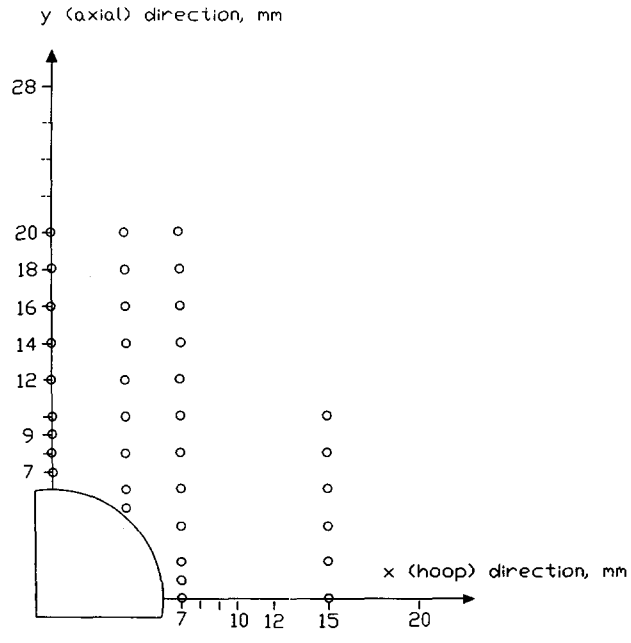

Figure 5 Loci of residual stress measurement positions surrounding the defect. All measurements were taken from a region just below the outside wall surface

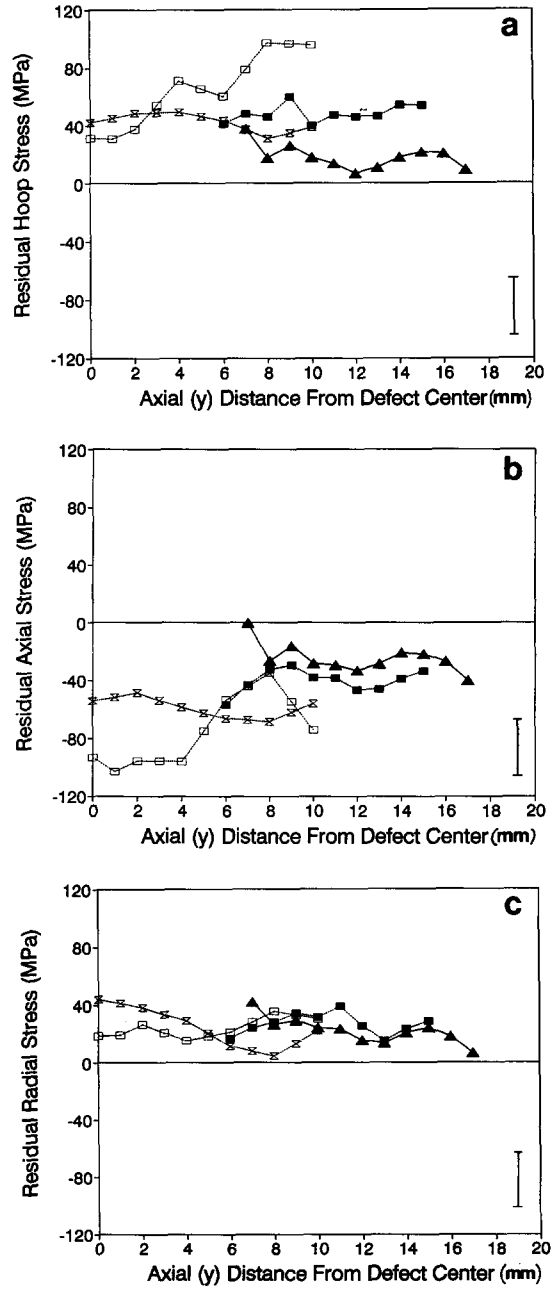

Figure 6 Experimentally determined residual hoop (a), axial (b) and radial (c) stresses (uncertainty ~ ±20 MPa, shown as a single error bar on graph). Each symbol represents a different × (hoop) position: 0 mm -▲-; 4 mm -■-; 7 mm -×-; 15 mm -□-

with the surface stresses shown in Figure 4 (measured >40 mm away from the defect) indicates that the residual hoop and axial stresses may vary by as much as 100 MPa across the outside pipe wall.

In the hoop and axial directions (Figures 6(a) and 6(b)) there appears to be some evidence that stress is reduced in the region immediately ahead of the defect, *ie* along the (y) axial direction at a hoop (x) position of 0 mm. This may represent some degree of stress relief associated with the defect milling procedure; however, given the significant variation of residual stress over the surface, this is not a conclusion that can be made with certainty.

Magnetic Barkhausen noise measurements

Figure 7 illustrates the change in MBN energy signal as a function of angle (with respect to the pipe axial direction), for the four surfaces through the pipe thickness. In all cases the largest signal arises when the applied magnetic field lies parallel to (or nearly parallel to) the axial direction, with the signal tapering off in a symmetrical fashion as the field is rotated towards the hoop (circumferential) direction. Differences in the MBN energy level are also observed between the four surfaces. Figure 8(a) shows the variation in the magnetic anisotropy parameter κ through the pipe thickness (note that an extra four surfaces were prepared at different locations through the pipe wall in order to obtain a more complete representation of κ *vs* depth). The variation of the background MBN signal as a function of defect depth is quantified in terms of the V_{rms} signal in Figure 8(b). These results are considered in more detail below.

General discussion

Texture and residual stresses in pipelines – the influence of processing

During its production a steel pipe is subjected to a number of different processing steps, some or all of which

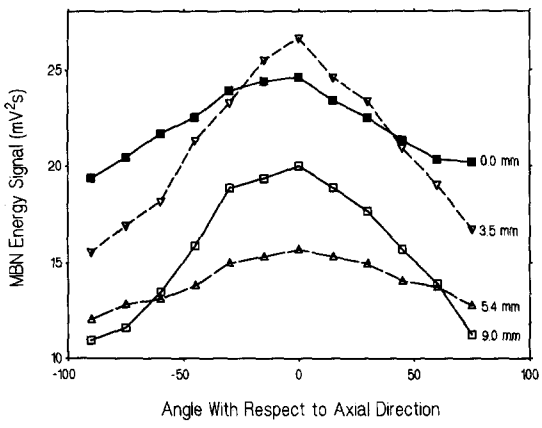

Figure 7 Variation of MBN as a function of angle (in degrees, with respect to the axial direction) for the four surfaces through the pipe wall thickness: outside surface (■——■); 3.5 mm below outside (▽——▽); 5.4 mm below outside (△——△); inside surface (□——□)

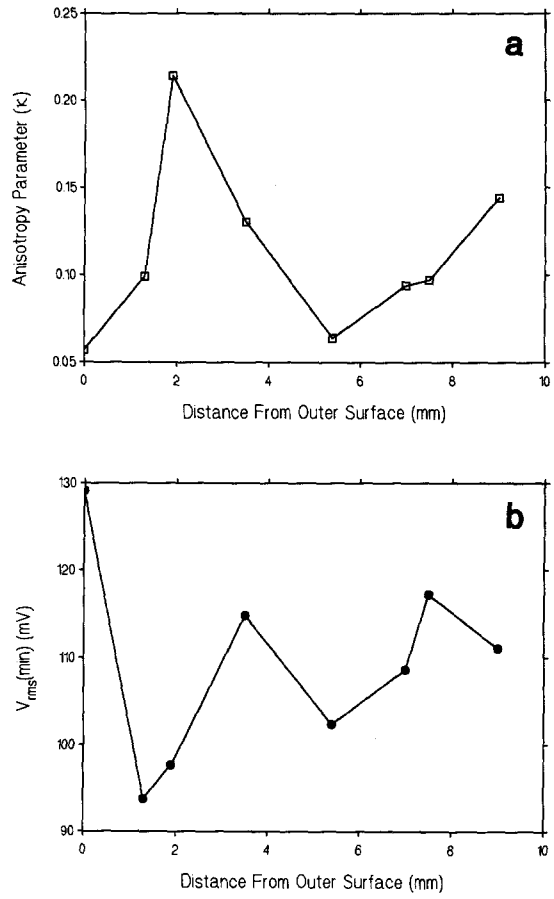

Figure 8 (a) Variation of κ through the pipe wall; (b) variation of V_{rms} (min) through the pipe wall

may introduce residual stresses which are retained in the finished product. In the first step, modern linepipe steel typically undergoes 'controlled rolling' to reduce steel slabs of ~10–20 cm thickness to plates 0.2–0.9 cm thick. Controlled rolling involves deformation of a steel slab within specific temperature intervals which correspond to certain microstructural phase stability regions, *ie* the austenite (γ) phase field above approximately 800°C and the ferrite (α) + Fe_3C phase field below 700°C, with the $\gamma + \alpha$ range lying between these two temperatures. The desired result is a uniform, recrystallized fine-grain structure throughout the plate thickness; this is achieved by ensuring that the finish tolling temperature (FRT) is close to the γ to α transition temperature. If this uniformly recrystallized structure is present then little or no residual stress would be expected following the rolling stage of the operation. This is not the case for the section of pipe in this study, with both X-ray pole figure and microstructural evidence indicating that the external pipe surfaces were unrecrystallized after rolling. Without stress relief in the form of recrystallization, these external surfaces of the plate (later pipe) are expected to remain in a state of axial compression[20], which is consistent with the residual axial stress result shown in Figure 4.

The strong axial residual compressive stress observed on the outside surface is probably associated with the deformed microstructure seen in Figure 1(b). The origin

of this deformation has not been determined, but it may have resulted from one of the pair of rolls rotating at a slightly higher speed than the other, causing a 'wrinkling' type of effect. Since the plate surface temperature was below the recrystallization temperature, compressive stresses resulting from this problem were not subsequently relieved. This periodic surface deformation is likely to be responsible for the significant variation of axial and hoop stress observed across the external pipe surface (Figures 6(a) and 6(b)).

After completion of rolling, the next processing step involves the formation of the plate into a section of pipe. In axially welded, large diameter pipe such as the one considered here, the formation of the plate into a cylinder typically involves a two-stage cold bending process. In the first stage a 'U-ing' press forms the plate into a U-shape, and in the subsequent stage a semicircular hollow die (an 'O-ing' press) is lowered to form the typical circular cross-section. At this point a small gap still exists between the two edges, and therefore a force is applied to hold the edges together for axial welding. Finally, hydraulic pressure is used to cold-expand the pipe; this increases the yield point and creates a more uniform stress state through the pipe wall[20]. In the present study the pipe sample is subjected to an additional processing step, since the pipe was subsequently cut to form a semicircular section. The combination of bending and subsequent cutting creates a distinctive residual hoop stress pattern through the pipe wall[20]. The development of this residual stress state is shown in Figure 9. When a bending force is applied, the stress through the pipe wall varies as shown schematically in Figure 9(a). Upon release of the applied stress, the elastically deformed regions are prevented from recovering fully to the unstrained condition, and remain (to a lesser degree) in their previous stress state. The outer and inner plastically deformed regions assume a state of residual elastic tension and compression, respectively, in order to balance the elastic stresses across the cross-section, obtained in Figures 9(b) and 9(c). Considering the number of complicating factors and the experimental error, Figure 9(c) compares favourably with the form of the experimentally determined residual hoop stress shown in Figure 4.

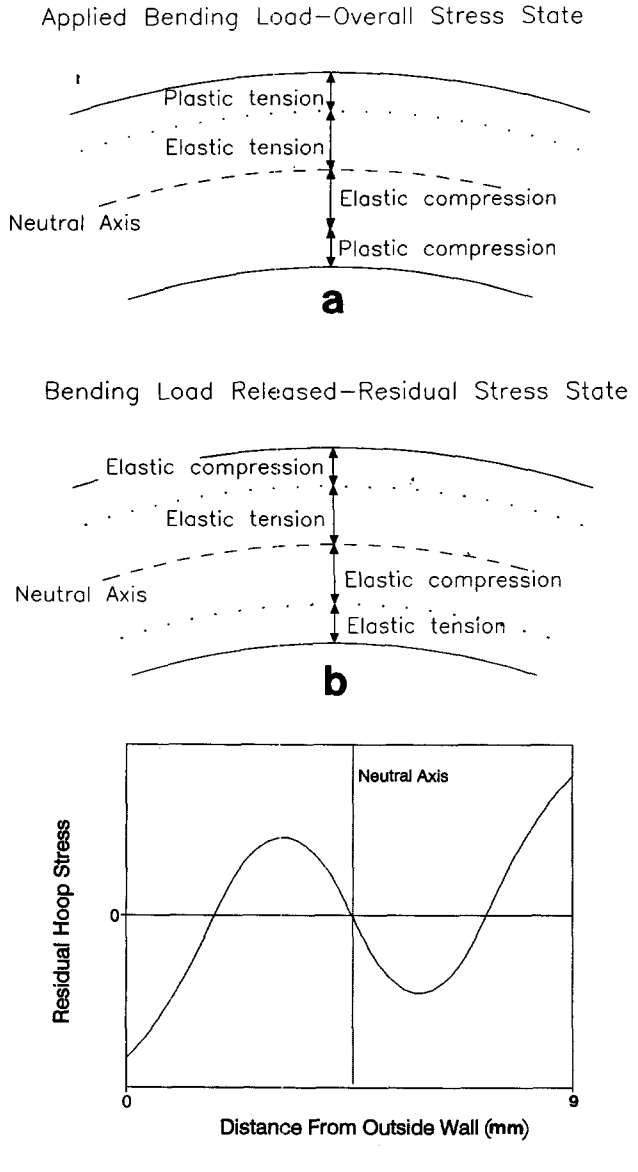

Figure 9 Schematic illustration of stress state in the pipe wall: (a) under an applied bending load; (b) residual stress with load released; (c) residual stress (schematic) *vs* position measured from the outside wall (as illustrated in (b))

Correlation of MBN with pipeline texture and residual stress

As discussed previously, magnetic behaviour is strongly dependent on crystallographic anisotropy. In recent studies of MBN *vs* orientation on strain-free transformer steel[21], we found relationships similar to those shown in Figure 7, with the maximum MBN energy signal obtained when the magnetizing field was parallel to the rolling direction; in these grain-oriented steels this corresponds to the ⟨100⟩ easy magnetization direction. One might therefore expect a correlation between the ⟨100⟩ direction and MBN in the pipeline steel specimen, provided it is strongly textured. In order to establish whether such a relationship exists, (100) orientation distribution function analysis was performed on the X-ray pole figure data for the four surfaces through the wall thickness. The resulting (100) pole figures (rotated so that the axial direction lies in the centre) are shown in Figure 10(a)–(d). Information regarding the volume fraction of (100) poles in each of the three directions was extracted from these figures and is included (as a percentage, for each of the four surfaces) in Table 2. Perhaps the most notable information displayed in this table is the similarity between the two inner surfaces (3.5 and 5.4 mm depths), and also between the two external surfaces (inside and outside); this similarity was also reflected in the pole figures of Figure 3. Examination of the MBN results of Figures 7 and 8, however, reveals no such similarities in the two inside or the two outside surface results. This does not rule out the possibility of a relationship between

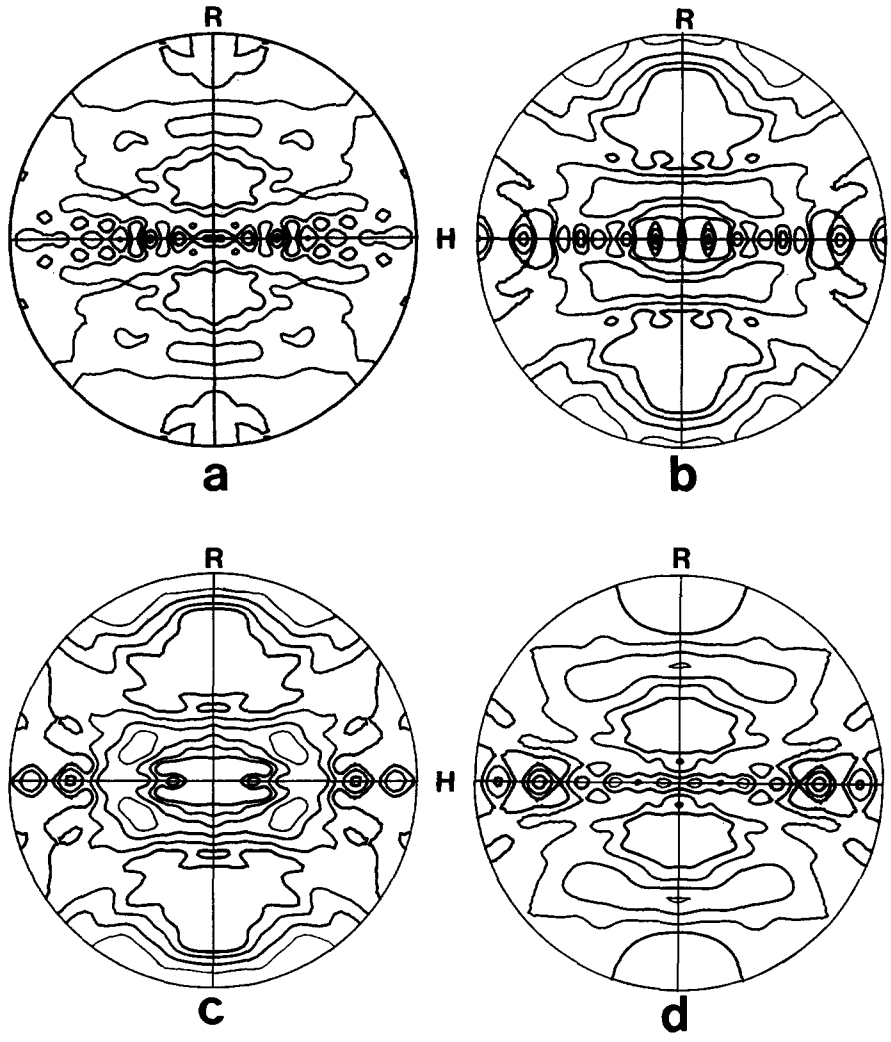

Figure 10 (100) pole figures (ODF-generated) for each of the four surfaces through the pipe wall thickness: (a) outside surface, (b) 3.5 mm below outside, (c) 6.0 mm below outside, (d) inside surface. H = hoop direction, R = radial direction, centre is axial direction

Table 2.

Depth below outside surface (mm)	Poles which are ⟨100⟩ in each direction (%)		
	Radial	Hoop	Axial
0 (outside wall)	10.3	11.5	13.9
3.5	14.1	9.5	9.3
5.4	15.1	9.2	8.7
9 (inside wall)	9.0	10.6	13.7

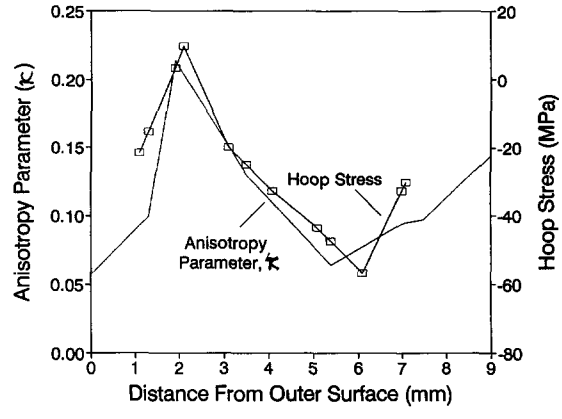

Figure 11 Comparison of κ and residual hoop stress variation through the pipe wall thickness

crystallographic texture and MBN in this sample; however, it is likely that the relationship is too complex to be determined by the type of MBN technique used in this study.

The relationship between MBN and elastic stress level can be made by comparing the MBN results of Figure 8 (again, through the thickness) with the residual stress results of Figure 4. An interesting correlation appears between the residual hoop stress result and the magnetic anisotropy parameter κ, as shown in Figure 11. According to previous work[18,21] the data observed in Figure 7 indicates that the magnetic easy axis in this pipe lies in the axial direction. The κ parameter therefore indicates the relative 'strength' of the easy axis in the

axial direction. As outlined in the introduction, the application of tensile stress in the hoop direction should tend to shift the easy magnetization direction towards the hoop, whereas hoop compression should reinforce the axial easy magnetization direction. According to this argument, an inverse relationship should be expected between the κ parameter and the hoop stress. Figure 11 indicates that the opposite appears to be true, *ie* the hoop stress appears to correlate directly with the κ parameter.

Several factors which have not been considered in the simple argument mentioned above may complicate the relationship between the measured through-wall hoop residual stress and the measured MBN signal. These factors include: (i) the effect of residual stresses and plastic deformation on the MBN signal; (ii) the precise relationship between the stress vector and its effect on both the magnitude and orientation of the magnetic easy axis as measured by MBN; (iii) the assumption that the position of the defect (at nine o'clock to the long seam weld) and the position on the pipe from which the MBN sample was cut (at 6 o'clock relative to the weld) have undergone similar processing; and (iv) that the MBN measurements were made on a small sample (17 mm × 17 mm × 2 mm) that had been cut from the pipe, and which was then further cut into slices with EDM so that, although no new residual stresses were introduced, residual stresses previously present in the pipe may have been relieved. Work is currently under way to further examine the influence of these factors on the MBN signal.

The observation of a low anisotropy (Figure 8(a)) but high background MBN V_{rms} signal (Figure 8(b)) at the outside surface of the pipe is correlated with observation of semicircular pearlite bands in the optical microscopy (Figure 2(b)) which was taken as indicative of compression-type plastic deformation, and unrecrystallized shear-type texture associated with the rolling process indicated in the (110) X-ray pole results shown in Figure 3(a). Both the microscopy results and the X-ray results at the surface may be taken as evidence for the presence of residual strains[5]. These surface conditions may be associated with surface processing as discussed earlier. It is possible, therefore, to interpret the reduction in the anisotropy and the overall increase in the background MBN signal on the outside surface as that due to a processing-induced secondary magnetic easy axis oriented at 90° to the majority easy axis direction which is in the pipe axial direction.

Summary and conclusions

The objective of this study was to characterize the crystallographic texture, microstructure and residual stresses in a sample of 610 mm diameter X70 pipeline steel and to correlate these properties with magnetic Barkhausen noise (MBN) measurements. The MBN measurements may be used in the nondestructive characterization of the magnetic behaviour of the pipeline steel which is a prime factor in determining MFL signals during pipeline inspection. The texture and microstructural results indicated that during rolling the temperature was insufficient to facilitate recrystallization at the external plate surface, resulting in significant residual (axial) compressive stresses at the outer pipe wall. The experimentally measured residual hoop stresses through the thickness of the pipe wall were consistent with that expected from cold bending followed by relaxation (*ie* cutting the section). MBN *vs* orientation measurements on sections through the thickness consistently produced the largest noise signal in the axial direction, indicating that the magnetic easy axis lies along the pipe axis. Although previous work on a less complex steel[21] found a strong correlation between MBN and the ⟨100⟩ direction, a similar relationship could not be found for this pipeline section, where the crystallographic texture is less well defined. A correlation was found between residual hoop stress and κ; however, more work needs to be done to clarify the origin of this relationship. A large background MBN signal along with a low MBN anisotropy value, κ, was correlated with unrecrystallized texture and surface plastic deformation.

In summary, this work shows something of the complexity of the effects of metallurgical structure and multiple residual stresses on the magnetic behaviour of a typical highly engineered pipeline steel.

Acknowledgement

This research was supported by the Natural Sciences and Engineering Council of Canada and Pipetronics.

References

1 **Atherton, D.L.** 'Design of magnetic flux leakage detectors for pipeline applications' *Proc. 3rd Nat. Seminar on Nondestructive Evaluation of Ferromagnetic Materials, Houston, Texas* (1988)
2 **Atherton, D.L.** 'Effect of line pressure on the performance of magnetic inspection tools for pipelines' *Oil Gas J* **84** (43) (October 1986) pp 86–89
3 **Kiefner, J.F. and Vieth, P.H.** 'A modified criterion for evaluating the remaining strength of a corroded pipe' *Project PR3-805: Pipeline Research Committee, American Gas Association* (1989)
4 **Tietsma, A.** 'Pipeline inspection by intelligent high resolution and conventional magnetic flux leakage pigs' *Proc. Int. Conf. on Pipeline Reliability, Calgary, Canada* (June 1992)
5 **Cullity, B.D.** *Introduction to Magnetic Materials* Addison-Wesley, Reading, MA (1972) p 208
6 **Atherton, D.L., Dhar, A., Hauge, C. and Laursen, P.** 'Effects of stress on magnetic flux leakage indications from pipeline inspection tools' *Oil Gas J* **90** (1992) p 81
7 **Laursen, P. and Atherton, D.L.** 'Effects of line pressure stress on magnetic flux leakage flux patterns' *Br J Nondestr Testing* **34** (1992) pp 285–288
8 **Clapham, L., Krause, T., Olsen, H., Ma, B., Atherton, D.L. and Holden, T.M.** 'The application of neutron diffraction to stress mapping around a blind-hole defect in stressed pipeline steel' *J Strain Anal Eng Des* **29** (1994) pp 317–323
9 **Holden, T.M., Root, J.H., Fidleris, V., Holt, T.A. and Roy, G.** 'Application of neutron diffraction to engineering problems II' *Materials Science Forum* **27/28** (1988) pp 359–370
10 **Krawitz, A.D. and Holden, T.M.** *Mat Res Soc Bull* **15** (1990) p 57
11 **Kroner, E.** 'Berechnung der elastichen Konstanten des Vielkristalls aus den Konstanten des Einkristalls' *Z Physik* **151** (1958) p 504
12 **Behnken, H. and Hauk, V.** 'Berechnung der Röntgenographischen Elastizitatskonstanten (REK) des Vielkristalls aus den Einkristalldaten für beliebige Kristallsymmetrie' *Z Metallkunde* **77** (1986) p 620

13 **Dever, D.J.** 'Temperature dependence of the elastic constants in α-iron single crystals: relationship to spin order and diffusion anomalies' *J Appl Phys* **43** (1972) p 2393
14 **Tiitto, S.** 'On the influence of microstructure on magnetization transitions in steel' *Acta Polytech Scand, Appl. Phys. Ser.* **119** (1977) pp 3–80
15 **Clapham, L., Jagadish, C. and Atherton, D.L.** 'The influence of pearlite on Barkhausen noise generation in plain carbon steels' *Acta Metall Mater* **39** (7) (1991) pp 1555–1562
16 **Titto, K.** 'Use of Barkhausen effect in testing for residual stresses and material defects' *Non-destr Test Austral* **26** (2) (March/April 1989) pp 36–41
17 **Gardner, C.G., Matzakanin, G.A. and Davidson, D.L.** 'The influence of mechanical stress on magnetization processes and Barkhausen jumps in ferromagnetic materials' *Intern J Nondestr Test* **3** (2) (1971) pp 131–169
18 **Dhar, A., Jagadish, C. and Atherton, D.L.** 'Using the Barkhausen effect to determine the easy axis of magnetization in steels' *Mater Eval* **50** (October 1992) pp 1139–1141
19 **Cullity, B.D.** *Elements of X-ray Diffraction* 2nd Edition, Addison-Wesley, Reading, MA (1978)
20 **Dieter, G.E.** *Mechanical Metallurgy* 3rd Edition, McGraw-Hill, New York (1986)
21 **Krause, T.W., Clapham, L. and Atherton, D.L.** 'Characterization of the magnetic easy axis in pipeline steel using magnetic Barkhausen noise' *J Appl Phys* **75** (1994) pp 7983–7988